Brief Communication

Cell Chemical Biology

Succinylation of a KEAP1 sensor lysine promotes NRF2 activation

Graphical abstract

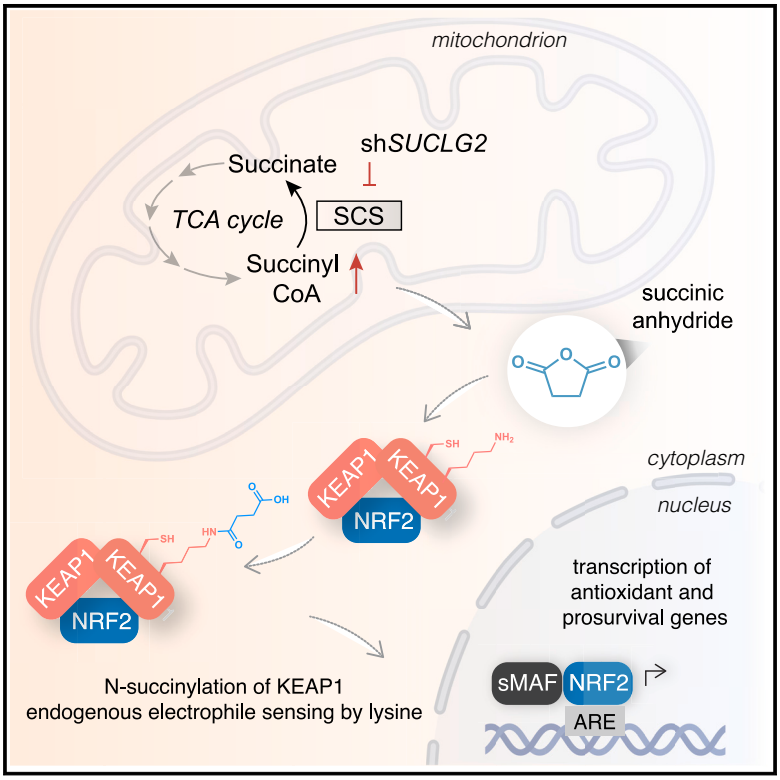

Highlights

- Loss of succinyl-CoA synthetase activates NRF2-driven transcription
- Elevated levels of succinyl-CoA byproduct, succinic anhydride, activate NRF2
- Succinic anhydride covalently and non-enzymatically modifies lysine 131 of KEAP1
- KEAP1 can sense electrophiles by a conserved sensor lysine residue

Authors

Lara Ibrahim, Caroline Stanton, Kayla Nutsch, ..., Gabriel C. Lander, R. Luke Wiseman, Michael J. Bollong

Correspondence

wiseman@scripps.edu (R.L.W.), mbollong@scripps.edu (M.J.B.)

In brief

NRF2 repressor protein KEAP1 senses exogenous and endogenous electrophilic chemicals through cysteine sensor residues. Ibrahim et al. identify the succinyl-CoA byproduct succinic anhydride as modifying a conserved lysine in KEAP1, indicating that lysine can serve an electrophile sensing role in this protein.

Ibrahim et al., 2023, Cell Chemical Biology *30*, 1–8
October 19, 2023
https://doi.org/10.1016/j.chembiol.2023.07.014

CellPress

Please cite this article in press as: Ibrahim et al., Succinylation of a KEAP1 sensor lysine promotes NRF2 activation, Cell Chemical Biology (2023), https://doi.org/10.1016/j.chembiol.2023.07.014

Cell Chemical Biology

CellPress

Brief Communication

Succinylation of a KEAP1 sensor lysine promotes NRF2 activation

Lara Ibrahim,[1,2] Caroline Stanton,[1,2] Kayla Nutsch,[2] Thu Nguyen,[2] Chloris Li-Ma,[2] Yeonjin Ko,[2] Gabriel C. Lander,[3] R. Luke Wiseman,[1,*] and Michael J. Bollong[2,4,*]

[1]Department of Molecular Medicine, Scripps Research, San Diego, CA 92037, USA
[2]Department of Chemistry, Scripps Research, San Diego, CA 92037, USA
[3]Department of Integrative Structural and Computational Biology, Scripps Research, San Diego, CA 92037, USA
[4]Lead contact
*Correspondence: wiseman@scripps.edu (R.L.W.), mbollong@scripps.edu (M.J.B.)
https://doi.org/10.1016/j.chembiol.2023.07.014

SUMMARY

Cross talk between metabolism and stress-responsive signaling is essential for maintaining cellular homeostasis. This cross talk is often achieved through covalent modification of proteins by endogenous, reactive metabolites that regulate key stress-responsive transcription factors like NRF2. Metabolites including methylglyoxal, glyceraldehyde 3-phosphate, fumarate, and itaconate covalently modify sensor cysteines of the NRF2 repressor KEAP1, resulting in stabilization of NRF2 and activation of its cytoprotective transcriptional program. Here, we employed a shRNA-based screen targeting the enzymes of central carbon metabolism to identify additional regulatory nodes bridging metabolism to NRF2 activation. Succinic anhydride, increased by genetic depletion of the TCA cycle enzyme succinyl-CoA synthetase or by direct administration, results in N-succinylation of lysine 131 of KEAP1 to activate NRF2 signaling. This study identifies KEAP1 as capable of sensing reactive metabolites not only by several cysteine residues but also by a conserved lysine residue, indicating its potential to sense an expanded repertoire of reactive metabolic messengers.

INTRODUCTION

The accumulation of intracellular reactive oxygen species (ROS), also referred to as oxidative stress, leads to the modification of cellular macromolecules including proteins, lipids, and nucleic acids and induces cellular dysfunction implicated in the onset and pathogenesis of many diseases.[1] Crucial to counteracting the damaging effects of ROS is the inducible transcriptional activity of nuclear factor erythroid 2-related factor 2 (NRF2).[2] This cap'n'collar (CNC) basic leucine zipper transcription factor (TF) serves as the primary stress-responsive transcription factor activated in response to oxidative stress and is responsible for inducing expression of antioxidant gene products to mitigate ROS-associated damage.[3] In unstressed cellular conditions, NRF2 is sequestered in the cytoplasm and constitutively ubiquitinated through interactions with its repressor protein and Cullin 3 (CUL3) E3 ligase adapter KEAP1 (Kelch-like ECH-associated protein).[4] In the presence of electrophilic xenobiotics or increased ROS, covalent modification of "sensor" cysteines in KEAP1 results in reduced NRF2 ubiquitination and degradation.[5] This stabilization allows NRF2 to translocate into the nucleus where it binds to antioxidant response elements (AREs) in the regulatory sequences of target genes involved in the maintenance of cellular redox, such as NAD(P)H quinone dehydrogenase 1 (NQO1). Dysregulated KEAP1-NRF2 activity is implicated in the pathogenesis of a wide range of diseases including neurodegeneration,[5] cancer,[6] inflammation,[7] and diabetes.[8] Accordingly, understanding the processes regulating KEAP1-NRF2 activity is critical for developing therapeutic strategies for treating a host of age-related diseases.

The modification of the NRF2-repressor and electrophile-sensor KEAP1 is of particular interest, as recent results have highlighted unique links between metabolism and KEAP1 modification in response to cellular stress. Numerous endogenous metabolites have been identified as signaling molecules, acting to directly modify KEAP1 "sensor" cysteines via covalent non-enzymatically derived posttranslational modifications. A common target residue is cysteine 151 within the BTB domain of KEAP1, which serves as a scaffold for the assembly of the CUL3-based E3 ligase complex that targets NRF2 for degradation.[9] Fumarate, an oncometabolite from the TCA cycle, has been shown to modify cysteine 151 of KEAP1 via S-succinylation-based modification.[10,11] Renal cell carcinomas often have mutations in fumarate hydratase, leading to the accumulation of fumarate, resulting in enhanced NRF2 activity and tumor progression.[10] Another TCA-derived metabolite, itaconate, has been found to alkylate cysteine 151 in KEAP1 and activate NRF2.[12,13] Intriguingly, the anti-inflammatory capacity of itaconate in macrophages requires the obligate activation of NRF2, highlighting the functional importance of itaconate-dependent KEAP1 modification.

More recently, evidence of reactive metabolites serving as signaling molecules to the KEAP1-NRF2 axis has come from two unbiased, high-throughput reporter-based screens which identified non-covalent pharmacological activators of NRF2.

Please cite this article in press as: Ibrahim et al., Succinylation of a KEAP1 sensor lysine promotes NRF2 activation, Cell Chemical Biology (2023), https://doi.org/10.1016/j.chembiol.2023.07.014

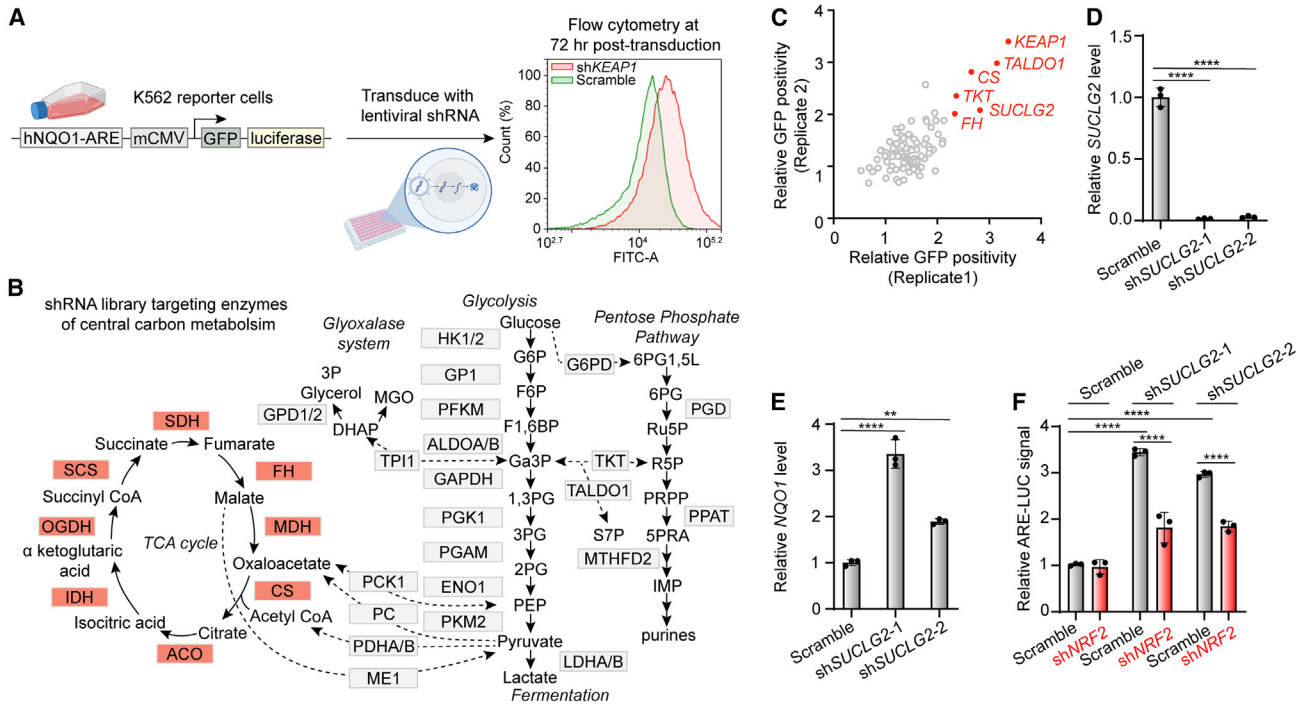

Figure 1. Loss of succinyl-CoA synthetase activates NRF2 driven transcription

(A) Schematic of the cellular screening platform using ARE-GFP-LUC K562 reporter cells. Shown is a representative plot indicating positivity for GFP after transduction with an shRNA targeting *KEAP1*.

(B) Schematic depicting the enzymes of central carbon metabolism targeted by the shRNA screen (boxes).

(C) Replicate fold increases in percent GFP positive ARE-GFP-LUC K562 cells after a 72 h exposure to the indicated shRNAs of the screen.

(D and E) Relative transcript levels of *SUCLG2* (D) and *NQO1* (E) after 48 h transient transfection of HEK293T cells with shRNAs targeting *SUCLG2* (n = 3; mean and s.d.; ****$p < 0.0001$, **$p < 0.01$, one-way ANOVA).

(F) Relative luminescence values of ARE-LUC reporter activity 72 h after transduction of lentiviruses encoding shRNAs to *SUCLG2* and *NRF2* in ARE-GFP-LUC K562 (n = 3; mean and s.d.; ****$p < 0.0001$, two-way ANOVA).

The identified small molecules, CBR-470-1[14] and sAKZ692,[15] were found to inhibit the glycolytic enzymes phosphoglycerate kinase 1 (PGK1) and pyruvate kinase (PKM2) resulting in the accumulation of the glycolytic metabolites methylglyoxal (MGO) and glyceraldehyde 3-phosphate (Ga3P), respectively. Mechanistic analyses indicated that these metabolites activate NRF2 through distinct mechanisms, involving two previously unidentified, non-enzymatically derived posttranslational modifications of KEAP1. MGO accumulation results in intramolecular crosslinks between cysteine 151 and arginine 15 or arginine 135 of neighboring KEAP1 molecules, inducing covalent KEAP1 dimerization and increased NRF2 activity.[14] In contrast, Ga3P induces S-lactoylation of cysteine 273 of KEAP1, which stabilizes NRF2 and promotes its transcriptional activation.[15] These results highlight key links between metabolic pathways and KEAP1-NRF2 signaling that are important for broadly coordinating metabolic and antioxidant regulation in response to diverse types of cellular insults.

The aforementioned results indicate that due to the virtue of their chemical structures or their positions within a given metabolic pathway, some reactive metabolites have likely been evolutionarily selected to relay metabolic information to the stress-sensing machinery of the cell. Given the observed capacity of several central metabolites to modify KEAP1 covalently, we hypothesized that several other conserved nodes throughout central carbon metabolism might also signal to the oxidative stress-sensing machinery. To test this hypothesis, we performed an shRNA screen of genes of the TCA cycle, glycolysis, the pentose phosphate pathway, and the glyoxalase system to identify if decreasing a specific enzymatic activity of one of these enzymes might increase the levels of a KEAP1 reactive metabolite capable of activating NRF2. Here, we show that genetic perturbations of the TCA cycle promote NRF2 activation through the non-enzymatic N-succinylation of a regulatory lysine in the BTB domain of KEAP1. These results demonstrate a new posttranslational mechanism by which KEAP1 can sense metabolic disruptions, further linking the status of cellular metabolic health to the activation of the NRF2 antioxidant signaling pathway.

RESULTS

Succinyl-CoA synthetase depletion activates NRF2 transcriptional signaling

To identify potential metabolic regulators of NRF2 activity, we screened shRNAs against known metabolic enzymes to identify those whose depletion induced NRF2 activation. Toward that aim, we transduced K562 lymphoblast cells with the NRF2 reporter plasmid ARE-GFP-LUC, which encodes the NRF2 ARE-binding site from the promoter of the human *NQO1* gene driving the expression of GFP and luciferase (Figure 1A). This enables

Please cite this article in press as: Ibrahim et al., Succinylation of a KEAP1 sensor lysine promotes NRF2 activation, Cell Chemical Biology (2023), https://doi.org/10.1016/j.chembiol.2023.07.014

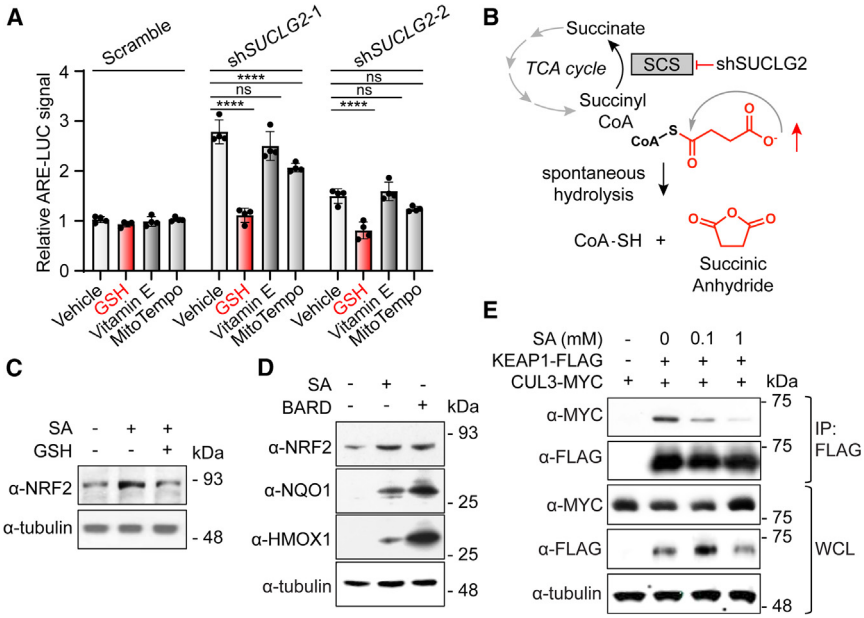

Figure 2. Augmented levels of succinic anhydride activate NRF2 signaling

(A) Relative ARE-LUC reporter activity induced shRNAs targeting *SUCLG2* in ARE-GFP-LUC K562 cells in the presence of the indicated antioxidants (10 mM each; n = 4; mean and s.d.; ns = not significant $p > 0.05$, ****$p < 0.0001$, two-way ANOVA).

(B) Schematic depicting the increase of succinyl-CoA and subsequent spontaneous formation of SA after knock down of the SCS subunit *SUCLG2*.

(C) Representative Western blotting for NRF2 levels after 4 h treatment of HEK293T cells with SA (10 mM) in the absence or presence of GSH (10 mM).

(D) Representative Western blots of NRF2, NQO1, and HMOX1 levels from IMR32 cells treated with SA (0.1 mM) or bardoxolone (BARD; 250 nM).

(E) Representative anti-MYC Western blotting of anti-FLAG coimmunoprecipitated material after 1 h of SA treatment in HEK293T expressing MYC-CUL3 and KEAP1-FLAG transgenes.

the measurement of NRF2 activation by GFP fluorescence or by luciferase activity. Monoclonal cells expressing this reporter were then transduced with shRNA targeting *KEAP1*, and after 72 h, we selected the cell line with the most dynamic and reproducible induction of the GFP signal measured by flow cytometry. We then transduced reporter cells with shRNAs-targeting genes encoding 30 metabolic enzymes (3 shRNAs/gene) of glycolysis, the pentose phosphate pathway (PPP), the glyoxalase system, or the TCA cycle (Figure 1B). We then measured ARE-GFP reporter activity by flow cytometry (Figure 1C). This approach identified genes whose depletion is known to increase intracellular levels of reactive metabolites capable of activating NRF2. For example, depletion of fumarate hydratase (FH) was identified as a top hit in the screen, activating the ARE-GFP reporter, consistent with studies showing fumarate hydratase deficiency increases cellular levels of the KEAP1-reactive metabolite fumarate.[10,11,16] Further, depletion of transketolase (TKT) or transaldolase (TALDO1), two enzymes in the non-oxidative branch of the PPP, also resulted in ARE-GFP reporter activation. This result likely reflects the ability for these enzymes to reversibly catalyze reactions with the glycolytic metabolite Ga3P, which we have previously shown to activate NRF2 through direct modification of KEAP1.[15] Collectively, these results confirm the ability of our approach to identify links between perturbations of metabolic pathways and NRF2 activation.

Interestingly, the depletion of *SUCLG2*, a subunit of succinyl-coA synthetase (SCS) enzyme complex of the mitochondrial TCA cycle also activated the ARE-GFP reporter (Figure 1C). The magnitude of reporter activation, like that induced by depletion of other enzymes, was dependent on the amount of transduced lentiviral shRNA, indicating dose-dependent activation (Figure S1A). Depletion of *SUCLG2* by two distinct shRNAs was confirmed by qPCR in HEK293T cells (Figure 1D). We demonstrated that depletion of *SUCLG2* increased expression of the NRF2 target gene *NQO1* in HEK293T cells by qPCR (Figure 1E). Further, *SUCLG2* depletion was also shown to increase luciferase activity in K562 cells expressing this dual reporter (Figures 1A and 1F). Knock down of *NRF2* inhibited the increase in ARE-luciferase activity induced by *SUCLG2* depletion, confirming that this activation reflects NRF2-dependent transcriptional activation (Figure 1F). The ability of *SUCLG2* depletion to activate reporter activity was observed in cells grown in glucose or galactose-containing media (Figure S1B), indicating that this effect is independent of the source of cellular ATP. Knock down of the other subunits of the SCS enzyme complex, *SUCLG1* and *SUCLA2*, also increased ARE reporter activity in HEK293T cells, albeit to a lesser degree than *SUCLG2* (Figure S1C). Loss of SUCLG2 was not found to decrease the proliferation or number of viable K562 reporter cells or HEK293T cells (Figures S1D and S1E). Interestingly, SUCLG2 depletion did decrease cellular ATP levels, while statistically augmenting the levels of GTP, a result consistent with a potential decrease in TCA activity via the loss of a GTP-consuming enzyme, although labile heme levels (a downstream product of succinyl-CoA metabolism) were unaffected by SUCLG2 loss (Figures S1F–S1H). Collectively, these results show that depletion of *SUCLG2* and likely the SCS complex activates NRF2 transcriptional signaling in multiple cell types, revealing a new link between mitochondrial TCA activity and NRF2 activation.

Succinic anhydride activates NRF2

We next sought to identify if increased levels of a reactive metabolite were responsible for NRF2 activation induced by *SUCLG2* depletion. We demonstrated that ARE-luciferase activity induced by *SUCLG2* depletion is decreased by treatment of the thiol-containing antioxidant glutathione (GSH) or N-acetyl cysteine (NAC; Figures 2A and S1I). However, the general antioxidant vitamin E did not reduce ARE-luciferase reporter activity, while the mitochondrial-targeted antioxidant MitoTEMPO showed only a mild reduction in reporter activation. These results are consistent with a model in which *SUCLG2* depletion

Please cite this article in press as: Ibrahim et al., Succinylation of a KEAP1 sensor lysine promotes NRF2 activation, Cell Chemical Biology (2023), https://doi.org/10.1016/j.chembiol.2023.07.014

increases the concentration of a reactive metabolite that could activate NRF2 through KEAP1 modification.

Depletion of SCS leads to increased levels of succinyl-CoA and global protein N-succinylation.[17] Further, reactive acyl-CoA metabolites are known to traverse the mitochondrial membranes and non-enzymatically acylate and succinylate lysines and cysteines on cytosolic proteins.[18,19] This suggests that increases in succinyl-CoA induced by *SUCLG2* depletion could contribute to NRF2 activation observed under these conditions (Figure 2B). Previous studies indicate that succinyl-CoA self-hydrolyzes to generate free coenzyme A and the highly reactive cyclic byproduct succinic anhydride, which has been shown to be the most likely mechanism of protein succinylation.[20] We hypothesized that the knock down of *SUCLG2* leads to increased levels of succinic anhydride (SA) that modify KEAP1 and subsequently activate NRF2 signaling (Figure 2B). Interestingly, treatment with SA stabilized NRF2 in HEK293T cells, while co-treatment with GSH decreased this stabilization (Figure 2C). We confirmed that SA can result in the S-succinylation of GSH, as monitored by LC-MS/MS (Figure S2A). Western blotting experiments additionally confirmed that SA treatment of IMR32 cells also stabilizes NRF2 to a similar level to the clinical stage pharmacological NRF2 activator bardoxolone methyl (BARD), resulting in the downstream increase in protein levels of the NRF2 target genes NQO1 and heme oxygenase 1 (HMOX1, Figure 2D). To further define the impact of SA on NRF2 stabilization, we monitored the association between KEAP1-FLAG and MYC-CUL3—the ligase that targets NRF2 for degradation—in HEK293T cells. We observed dose-dependent reductions in recovered MYC-CUL3 in KEAP1-FLAG immunoprecipitations, indicating that SA disrupted the interaction between KEAP1 and CUL3 (Figure 2E), the canonical route by which pharmacological modification of KEAP1 leads to NRF2 activation. Treatment with SA also activated the ARE reporter in K562 cells (Figures S2B and S2C). Importantly, neither *SUCLG2* knockdown nor SA treatment increased reactive oxygen species (ROS) in K562 cells, as measured by DCFDA (Figure S2D). These results indicate that SA activates NRF2 signaling through a mechanism independent of inducing oxidative stress, instead likely acting by covalently modifying KEAP1.

SA increases lysine succinylation on KEAP1

We next sought to identify the potential posttranslational modification of KEAP1 formed by SA. We employed a succinic anhydride probe molecule containing an alkyne reactivity handle (SA-alkyne) compatible with click chemistry-based conjugation to monitor KEAP1 modification (Figure 3A). We confirmed that SA-alkyne activates the ARE-luciferase reporter in IMR32 cells to a similar extent to that observed with SA (Figure 3B). Treatment of HEK293T cells overexpressing KEAP1-FLAG with increasing concentrations of SA-alkyne significantly increased the accumulation of modified KEAP1 identified in anti-FLAG-based immunoprecipitation experiments (Figure 3C). Critically, SA-alkyne modification of KEAP1 was competed by increasing concentrations of SA, confirming that SA covalently modifies KEAP1 (Figure 3D).

KEAP1 activity is primarily regulated through covalent modification of cysteine residues, most notably cysteine 151. To determine whether SA activates NRF2 through covalent modification of cysteine 151, we overexpressed wild-type KEAP1-FLAG or C151 A/S KEAP1-FLAG in IMR32 cells and monitored ARE-luciferase activation. Surprisingly, we found that mutation of C151 did not disrupt SA-dependent ARE-luciferase activation, suggesting that SA modifies KEAP1 on a different residue (Figure 3E). SA has previously been shown to modify lysine residues in proteins. To determine if SA also modifies lysine residues within KEAP1, we employed an antibody that detects lysine N-succinylation, evaluating if anti-FLAG immunoprecipitated KEAP1-FLAG displayed immunopositivity to increasing SA levels. Not only did exogenous SA treatment increase global succinylation of proteins, as anticipated, (Figure 3F), but we also observed dose-dependent increases of lysine succinylation in KEAP1-FLAG immunopurified from SA-treated cells (Figure 3F). *SUCLG2* depletion also increased lysine succinylation on KEAP1-FLAG in HEK293T cells co-treated with ET-29 (Figure 3G)—an inhibitor of the principle intracellular lysine desuccinylase SIRT5 that stabilizes succinylated lysines (Figure S3A).[21] Further, we found that treatment of HEK293T cells with SA increased lysine succinylation of endogenous KEAP1 (Figure S3B). Similar results were observed in reactions with recombinant KEAP1 and either SA or succinyl-coA (Figures S3C and S3D).

Lysine 131 succinylation functionally inhibits KEAP1 activity

The aforementioned results demonstrate that treatment with SA or *SUCLG2* depletion increases lysine succinylation on KEAP1. Next, we wanted to determine if this modification was functionally important to NRF2 activity. To identify the specific lysine residues of KEAP1 modified by SA, we used MS/MS analysis of KEAP1-FLAG immunoprecipitated from HEK293T cells treated with SA (Figures 4A and S4A). This effort identified lysine 131 of the BTB domain of KEAP1 as the principal lysine modified by this metabolite. Lysine succinylation of residue 131 was also observed from recombinant KEAP1 preparations treated with SA (Figures S4B and S4C). Importantly, overexpression of K131A KEAP1 decreased labeling by SA-alkyne (Figure 4B) and reduced KEAP1 lysine succinylation in SA-treated HEK293T cells (Figure 4C). Overexpressed KEAP1-containing mutations in the key electrophile sensing residue C151 did not affect these modifications. This indicates that K131 is the primary site of lysine succinylation on KEAP1.

Although K131 exists in a flexible disordered region that exhibits weak electron density in structural models,[22] this lysine residue appears uniquely positioned within a basic pocket that surrounds the key electrophile sensor reside C151 (Figure S4D).[23] This suggests that K131 succinylation may directly impact KEAP1 activity, and thus NRF2 activation. Consistent with this, we found that K131A KEAP1 blocked SA-dependent activation of the ARE-luciferase reporter, while C151S KEAP1 did not (Figure 4D). This contrasts with established NRF2 activators like bardoxolone that activate NRF2 through C151 modification (Figure S4E). Collectively, these results indicate that SA-dependent succinylation of KEAP1 at residue K131 regulates NRF2 activation.

DISCUSSION

To comprehensively map the interactions between reactive metabolites and the oxidative stress sensing machinery of the cell,

Please cite this article in press as: Ibrahim et al., Succinylation of a KEAP1 sensor lysine promotes NRF2 activation, Cell Chemical Biology (2023), https://doi.org/10.1016/j.chembiol.2023.07.014

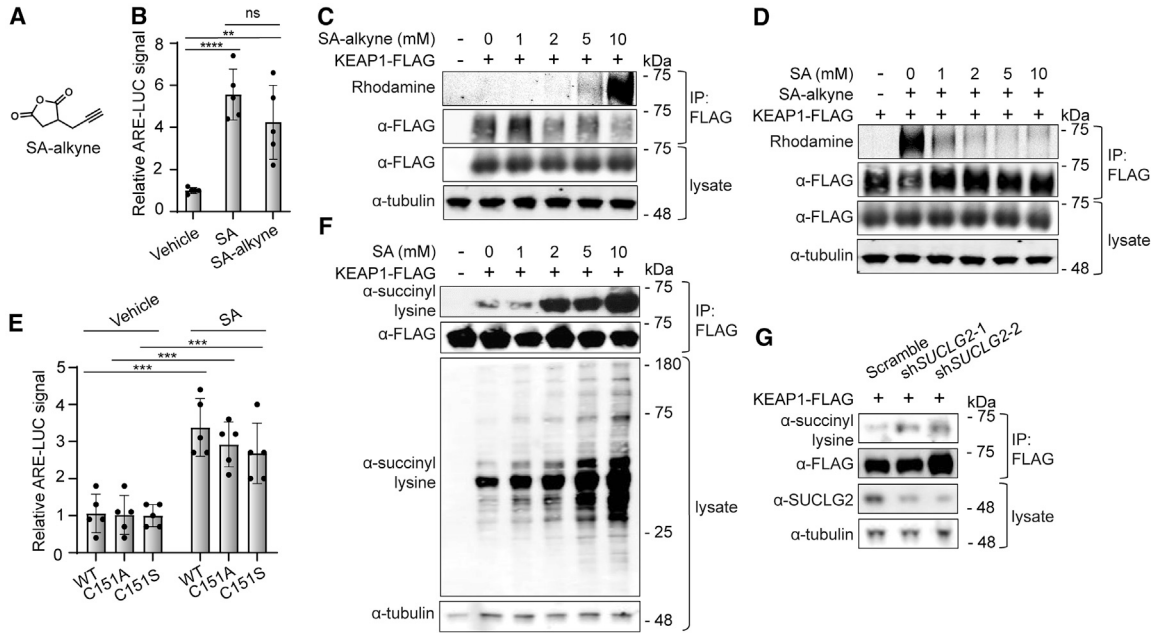

Figure 3. SA accumulation leads to covalent modification of KEAP1 lysines

(A) Structure of succinic anhydride alkyne (SA-alkyne).

(B) Relative luminescence values of ARE-LUC reporter activity from IMR32 cells treated with SA or SA-alkyne (12 mM) for 4 h (n = 5, mean and s.d.; ****$p < 0.0001$, **$p < 0.01$, one-way ANOVA).

(C) Representative fluorescence scan of rhodamine azide labeling of anti-FLAG immunoprecipitated material after treatment of HEK293T cells expressing KEAP1-FLAG with the indicated concentrations of SA-alkyne for 1 h.

(D) Representative fluorescence scan of rhodamine azide labeling of anti-FLAG immunoprecipitated material after pretreatment with the indicated concentrations of SA followed by a 1 h labeling with SA-alkyne (10 mM) in HEK293T cells expressing KEAP1-FLAG.

(E) Relative ARE-LUC activity from IMR32 cells expressing the indicated KEAP1 mutant and MYC-NRF2 and then treated with 1 mM SA for 4 h (n = 5; mean and s.d.; ***$p < 0.001$, two-way ANOVA).

(F) Western blotting for anti-N-succinyl lysine positivity of anti-FLAG immunoprecipitated material from HEK293T cells expressing KEAP1-FLAG after 1 h treatment with the indicated concentrations of SA.

(G) Western blotting for anti-N-succinyl lysine positivity of anti-FLAG immunoprecipitated material from HEK293T cells expressing KEAP1-FLAG and shRNAs targeting *SUCLG2*, stabilized by the desuccinylase inhibitor ET-29 (10 μM).

here we have conducted an shRNA screen of the enzymes in central carbon metabolism, targeting genes involved in glycolysis, the TCA cycle, the PPP, and the glyoxalase system. This effort identified the mitochondrial enzyme succinyl-CoA synthetase (SCS) as a key regulator of NRF2 activity, as genetic depletion of SCS leads to the N-succinylation of KEAP1 lysine 131 and subsequent NRF2 activation. The human KEAP1 protein contains 27 cysteines with at least 11 of them having been shown to play sensing roles, capable of being alkylated by exogenous electrophilic chemicals, resulting in the decreased ubiquitination of NRF2.[9] The molecular details by which covalent modification results in NRF2 activation have remained elusive; however, the consensus from the field suggests that relatively small posttranslational modifications of these cysteines most likely results in profound conformational changes in the KEAP1 intermolecular complex.[24] Here, we add evidence suggesting that in addition to this canonical cysteine sensing paradigm, that modifications to other sensor residues, like the lysine modification identified here, can additionally result in functional NRF2 activation.

Among the most targeted sensor cysteines in KEAP1 is cysteine 151 of the BTB domain, which has been shown to be covalently modified by numerous synthetic small molecules, including the clinically investigated oleananes, bardoxolone and omaveloxelone.[25] Notably, lysine 131 occupies a proximal site to cysteine 151 across the bardoxolone-binding cleft (6.3 Å apart in the crystal structure 4CXI).[22] Lysine 131, along with neighboring residues arginine 135 and lysine 150 have been shown to act as bases, locally repressing the pKa of cysteine 151, enabling its potent sensing of electrophilic chemicals.[23] To the extent that these neighboring basic residues may also increase the nucleophilicity of lysine 131 and enable its ability to sense electrophiles will necessarily be the work of future crystallographic and biochemical studies.

We have shown that lysine 131 modification in response to *SUCLG2* depletion is derived from the reactive byproduct of succinyl-CoA degradation, the metabolite succinic anhydride (SA). Importantly, several other mitochondrial metabolites have been shown to modify KEAP1, including fumarate and itaconate, both of which, like SA, are derived from the TCA cycle. Interestingly, KEAP1 has been shown to exist in two sensing forms, a cytoplasmic complex and one that is tethered to the outer face of the mitochondrial membrane via interactions with PGAM family member 5 (PGAM5).[26] These observations raise the intriguing possibility that this ternary complex of KEAP1, NRF2, and PGAM5 may provide a molecular sensing outpost for relaying specific mitochondrial metabolic information to the oxidative stress response.

Please cite this article in press as: Ibrahim et al., Succinylation of a KEAP1 sensor lysine promotes NRF2 activation, Cell Chemical Biology (2023), https://doi.org/10.1016/j.chembiol.2023.07.014

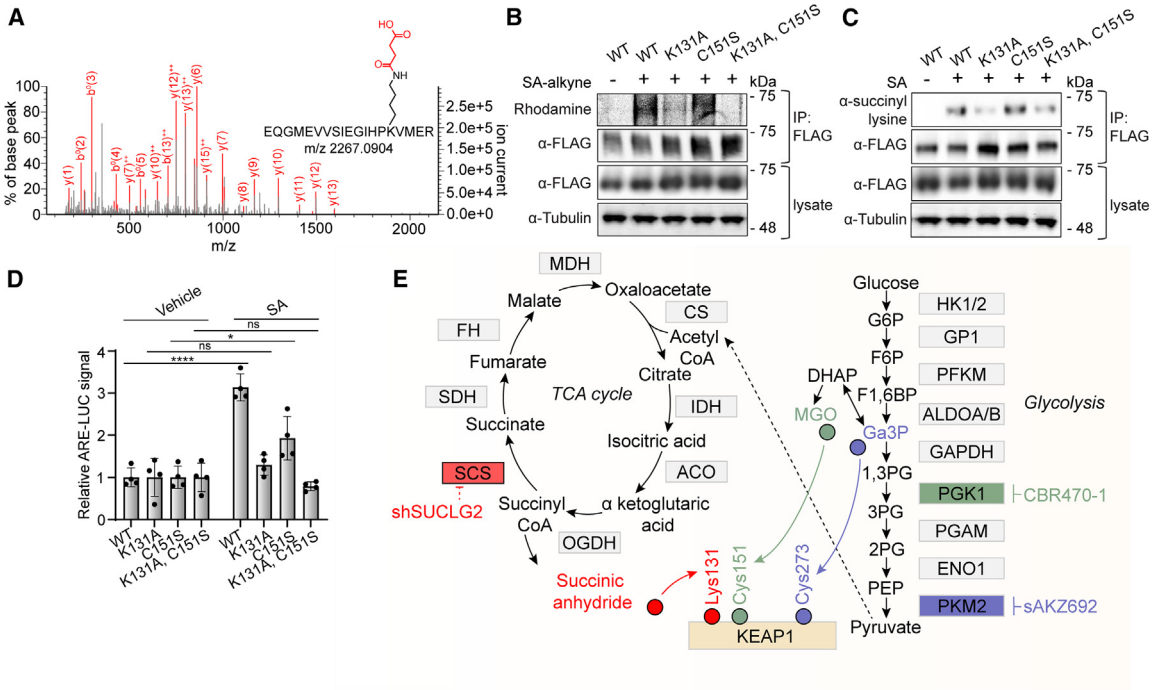

Figure 4. N-succinylation of Lysine 131 functionally inhibits KEAP1 activity

(A) MS/MS spectra of the N-succinylated K131 containing tryptic peptide immunoprecipitated from overexpressed KEAP1-FLAG from HEK293T cells treated with SA (10 mM).

(B) Representative fluorescence scan of rhodamine azide labeling of anti-FLAG immunoprecipitated material after pretreatment with the indicated concentrations of SA followed by a 1 h labeling with SA-alkyne (5 mM) in HEK293T cells expressing the indicated KEAP1-FLAG transgenes.

(C) Western blotting for anti-N-succinyl lysine positivity of anti-FLAG immunoprecipitated material from HEK293T cells expressing the indicated KEAP1-FLAG transgene mutants after 1 h treatment with SA (1 mM).

(D) Relative ARE-luciferase reporter activity from IMR32 cells expressing the indicated KEAP1-FLAG mutant transgenes and then treated with 1 mM SA for 4 h (n = 4; mean and s.d.; ns = not significant $p > 0.05$; ****$p < 0.0001$, *$p < 0.05$, two-way ANOVA).

(E) Schematic depicting metabolites from central carbon metabolism that can covalently modify the indicated residues on KEAP1.

The TCA cycle is a tightly regulated metabolic pathway using several feedback loops to maintain cellular homeostasis. Interestingly, succinyl-CoA levels have been shown to regulate the metabolic flux of the TCA cycle by inhibiting citrate synthase and α-ketoglutarate dehydrogenase through a negative feedback mechanism.[27] To the extent that increased succinyl-CoA levels might additionally serve as a sentinel for signaling TCA cycle imbalance to the oxidative stress-sensing machinery will be the work of future studies. In addition to SCS, we identified another TCA cycle enzyme as a hit from our screen, as genetic depletion of citrate synthetase (CS) was found to result in mean increase of 2.7-fold in ARE reporter activity (Figure 1C). CS catalyzes the formation of citrate from oxaloacetate (OA), a high-energy carbonyl-containing metabolite that is the product of the TCA cycle. Whether OA, and perhaps other carbonyl-containing metabolites of the TCA cycle might additionally be sensed by KEAP1 via posttranslational modifications of cysteines or lysines will be of keen interest in future work. Projecting forward, this work will provide the basis for understanding how these and other molecules maintain cellular homeostasis. Likewise, the lysine sensing-based mechanism described here might further inform efforts to covalently target KEAP1 with greater selectivity, potentially broadening the therapeutic scope of therapeutics aimed at activating NRF2 with increased tolerability.

Limitations of the study

Here we have shown that increased levels of succinic anhydride, either by its exogenous supplementation or by genetic depletion of SUCLG2, results in KEAP1 modification. These experiments were all performed in acute dosing paradigms, ranging from several hours to several days. It is conceivable that the cell may adapt to these physiological manipulations over time, a potential outcome that was not explored in this work. Additionally, experiments in this study were restricted to several cell lines. To the extent that modification of K131 might additionally occur in whole animals under certain physiological settings like metabolic stress or cancer will be of keen interest to future work.

SIGNIFICANCE

NRF2, a cap'n'collar transcription factor, serves as the master regulator of oxidative stress resistance in mammalian cells, augmenting cellular survival and manipulating metabolism in response to exogenous and endogenous electrophilic compounds. Accordingly, understanding the mechanisms by which NRF2 repressor protein KEAP1 senses electrophiles is of key physiological importance. Here, an shRNA-based screen of enzymes in central carbon metabolism revealed that loss of the TCA cycle enzyme

succinyl-CoA synthetase activates NRF2-driven transcription in cells. Mechanistic work identified the succinyl-CoA byproduct succinic anhydride as the relevant, reactive metabolite, acting to covalently modify a conserved lysine residue on KEAP1 to activate NRF2. In contrast to the 11 defined cysteine-based sensor residues in KEAP1, this study identifies a conserved lysine as essential in sensing the levels of an endogenous reactive electrophile. This work uncovers an electrophile sensing mechanism and is suggestive that KEAP1 is likely capable of sensing a broader repertoire of reactive metabolites. The finding that lysine modification functionally activates NRF2 may provide an avenue to identify pharmacological NRF2 activators with enhanced safety profiles for use as therapeutic agents.

STAR★METHODS

Detailed methods are provided in the online version of this paper and include the following:

- KEY RESOURCES TABLE
- RESOURCE AVAILABILITY
  - Lead contact
  - Materials availability
  - Data and code availability
- EXPERIMENTAL MODELS AND STUDY PARTICIPANT DETAILS
  - Cell lines
- METHOD DETAILS
  - Cloning
  - Lentivirus production and transduction
  - Stable cell line production
  - shRNA screen in ARE-GFP-LUC K562 reporter cells
  - ARE-LUC reporter assays
  - qRT-PCR
  - Quantification of ROS by DCFDA fluorescence
  - KEAP1-FLAG labeling experiments in HEK293T cells
  - Recombinant KEAP1 labeling *in vitro*
  - Immunoblotting
  - Endogenous KEAP1 immunoprecipitation
  - Quantification of cellular ATP, GTP, and heme
- QUANTIFICATION AND STATISTICAL ANALYSIS

SUPPLEMENTAL INFORMATION

Supplemental information can be found online at https://doi.org/10.1016/j.chembiol.2023.07.014.

ACKNOWLEDGMENTS

We thank Linh Truc Hoang of the Scripps Research Center for Metabolomics for assistance with mass spectrometry related experiments, and Zoe Adams of the Dawson Lab at Scripps Research for help with peptide synthesis. We also thank Nelson Wu of the Schief Lab at Scripps Research for advice regarding structural modeling. This work was supported by the NIH (GM146865 to MJB, DK107604 and AG046495 to RLW).

AUTHOR CONTRIBUTIONS

L.I., R.L.W., and M.J.B. designed research. L.I., T.N., C.L.M., and M.J.B. performed biochemical and cell-based biological experiments. K.N. and Y.K. purified recombinant protein. C.S. conducted mass spectrometry. L.I. analyzed data.

L.I., R.L.W., and M.J.B. wrote the paper. Financial support by the Skaggs Institute for Chemical Biology at Scripps Research.

DECLARATION OF INTERESTS

Declared none.

Received: April 27, 2023
Revised: July 4, 2023
Accepted: July 30, 2023
Published: August 23, 2023

REFERENCES

1. Forman, H.J., and Zhang, H. (2021). Targeting oxidative stress in disease: promise and limitations of antioxidant therapy. Nat. Rev. Drug Discov. *20*, 689–709. https://doi.org/10.1038/s41573-021-00233-1.
2. Ibrahim, L., Mesgarzadeh, J., Xu, I., Powers, E.T., Wiseman, R.L., and Bollong, M.J. (2020). Defining the Functional Targets of Cap'n'collar Transcription Factors NRF1, NRF2, and NRF3. Antioxidants *9*, 1025. https://doi.org/10.3390/antiox9101025.
3. Ma, Q. (2013). Role of Nrf2 in Oxidative Stress and Toxicity. Annu. Rev. Pharmacol. Toxicol. *53*, 401–426. https://doi.org/10.1146/annurev-pharmtox-011112-140320.
4. Sykiotis, G.P., and Bohmann, D. (2010). Stress-Activated Cap'n'collar Transcription Factors in Aging and Human Disease. Sci. Signal. *3*, re3.
5. Baird, L., and Yamamoto, M. (2020). The Molecular Mechanisms Regulating the KEAP1-NRF2 Pathway. Mol. Cell Biol. *40*, e00099-20. https://doi.org/10.1128/mcb.00099-20.
6. Rojo De La Vega, M., Chapman, E., and Zhang, D.D. (2018). NRF2 and the Hallmarks of Cancer. Cancer Cell *34*, 21–43. https://doi.org/10.1016/j.ccell.2018.03.022.
7. Saha, S., Buttari, B., Panieri, E., Profumo, E., and Saso, L. (2020). An Overview of Nrf2 Signaling Pathway and Its Role in Inflammation. Molecules *25*, 5474. https://doi.org/10.3390/molecules25225474.
8. Uruno, A., Yagishita, Y., and Yamamoto, M. (2015). The Keap1–Nrf2 system and diabetes mellitus. Arch. Biochem. Biophys. *566*, 76–84. https://doi.org/10.1016/j.abb.2014.12.012.
9. Sekhar, K.R., Rachakonda, G., and Freeman, M.L. (2010). Cysteine-based regulation of the CUL3 adaptor protein Keap1. Toxicol. Appl. Pharmacol. *244*, 21–26. https://doi.org/10.1016/j.taap.2009.06.016.
10. Adam, J., Hatipoglu, E., O'Flaherty, L., Ternette, N., Sahgal, N., Lockstone, H., Baban, D., Nye, E., Stamp, G.W., Wolhuter, K., et al. (2011). Renal Cyst Formation in Fh1-Deficient Mice Is Independent of the Hif/Phd Pathway: Roles for Fumarate in KEAP1 Succination and Nrf2 Signaling. Cancer Cell *20*, 524–537. https://doi.org/10.1016/j.ccr.2011.09.006.
11. Ooi, A., Wong, J.-C., Petillo, D., Roossien, D., Perrier-Trudova, V., Whitten, D., Min, B.W.H., Tan, M.H., Zhang, Z., Yang, X.J., et al. (2011). An Antioxidant Response Phenotype Shared between Hereditary and Sporadic Type 2 Papillary Renal Cell Carcinoma. Cancer Cell *20*, 511–523. https://doi.org/10.1016/j.ccr.2011.08.024.
12. Mills, E.L., Ryan, D.G., Prag, H.A., Dikovskaya, D., Menon, D., Zaslona, Z., Jedrychowski, M.P., Costa, A.S.H., Higgins, M., Hams, E., et al. (2018). Itaconate is an anti-inflammatory metabolite that activates Nrf2 via alkylation of KEAP1. Nature *556*, 113–117. https://doi.org/10.1038/nature25986.
13. Bambouskova, M., Gorvel, L., Lampropoulou, V., Sergushichev, A., Loginicheva, E., Johnson, K., Korenfeld, D., Mathyer, M.E., Kim, H., Huang, L.-H., et al. (2018). Electrophilic properties of itaconate and derivatives regulate the IκBζ–ATF3 inflammatory axis. Nature *556*, 501–504. https://doi.org/10.1038/s41586-018-0052-z.

14. Bollong, M.J., Lee, G., Coukos, J.S., Yun, H., Zambaldo, C., Chang, J.W., Chin, E.N., Ahmad, I., Chatterjee, A.K., Lairson, L.L., et al. (2018). A metabolite-derived protein modification integrates glycolysis with KEAP1-NRF2 signalling. Nature *562*, 600–604. https://doi.org/10.1038/s41586-018-0622-0.

15. Ko, Y., Hong, M., Lee, S., Kumar, M., Ibrahim, L., Nutsch, K., Sondermann, P., Sandoval, B., Bulos, M.L., Iaconelli, J., et al. (2023). S-lactoyl modification of KEAP1 by a reactive glycolytic metabolite activates NRF2 signaling. Proc. Natl. Acad. Sci. USA *120*. e2300763120. https://doi.org/10.1073/pnas.2300763120.

16. Noguchi, S., Ishikawa, H., Wakita, K., Matsuda, F., and Shimizu, H. (2020). Direct and quantitative analysis of altered metabolic flux distributions and cellular ATP production pathway in fumarate hydratase-diminished cells. Sci. Rep. *10*, 13065. https://doi.org/10.1038/s41598-020-70000-6.

17. Gut, P., Matilainen, S., Meyer, J.G., Pällijeff, P., Richard, J., Carroll, C.J., Euro, L., Jackson, C.B., Isohanni, P., Minassian, B.A., et al. (2020). SUCLA2 mutations cause global protein succinylation contributing to the pathomechanism of a hereditary mitochondrial disease. Nat. Commun. *11*, 5927. https://doi.org/10.1038/s41467-020-19743-4.

18. Lin, H., Su, X., and He, B. (2012). Protein Lysine Acylation and Cysteine Succination by Intermediates of Energy Metabolism. ACS Chem. Biol. *7*, 947–960. https://doi.org/10.1021/cb3001793.

19. Zhang, Z., Tan, M., Xie, Z., Dai, L., Chen, Y., and Zhao, Y. (2011). Identification of lysine succinylation as a new post-translational modification. Nat. Chem. Biol. *7*, 58–63. https://doi.org/10.1038/nchembio.495.

20. Wagner, G.R., Bhatt, D.P., O'Connell, T.M., Thompson, J.W., Dubois, L.G., Backos, D.S., Yang, H., Mitchell, G.A., Ilkayeva, O.R., Stevens, R.D., et al. (2017). A Class of Reactive Acyl-CoA Species Reveals the Non-enzymatic Origins of Protein Acylation. Cell Metabol. *25*, 823–837.e8. https://doi.org/10.1016/j.cmet.2017.03.006.

21. Du, J., Zhou, Y., Su, X., Yu, J.J., Khan, S., Jiang, H., Kim, J., Woo, J., Kim, J.H., Choi, B.H., et al. (2011). Sirt5 Is a NAD-Dependent Protein Lysine Demalonylase and Desuccinylase. Science *334*, 806–809. https://doi.org/10.1126/science.1207861.

22. Cleasby, A., Yon, J., Day, P.J., Richardson, C., Tickle, I.J., Williams, P.A., Callahan, J.F., Carr, R., Concha, N., Kerns, J.K., et al. (2014). Structure of the BTB Domain of Keap1 and Its Interaction with the Triterpenoid Antagonist CDDO. PLoS One *9*, e98896. https://doi.org/10.1371/journal.pone.0098896.

23. McMahon, M., Lamont, D.J., Beattie, K.A., and Hayes, J.D. (2010). Keap1 perceives stress via three sensors for the endogenous signaling molecules nitric oxide, zinc, and alkenals. Proc. Natl. Acad. Sci. USA *107*, 18838–18843. https://doi.org/10.1073/pnas.1007387107.

24. Holland, R., and Fishbein, J.C. (2010). Chemistry of the Cysteine Sensors in Kelch-Like ECH-Associated Protein 1. Antioxidants Redox Signal. *13*, 1749–1761. https://doi.org/10.1089/ars.2010.3273.

25. Dayalan Naidu, S., and Dinkova-Kostova, A.T. (2020). KEAP1, a cysteine-based sensor and a drug target for the prevention and treatment of chronic disease. Open Biol. *10*, 200105. https://doi.org/10.1098/rsob.200105.

26. Lo, S.-C., and Hannink, M. (2008). PGAM5 tethers a ternary complex containing Keap1 and Nrf2 to mitochondria. Exp. Cell Res. *314*, 1789–1803. https://doi.org/10.1016/j.yexcr.2008.02.014.

27. Martínez-Reyes, I., and Chandel, N.S. (2020). Mitochondrial TCA cycle metabolites control physiology and disease. Nat. Commun. *11*, 102. https://doi.org/10.1038/s41467-019-13668-3.

Please cite this article in press as: Ibrahim et al., Succinylation of a KEAP1 sensor lysine promotes NRF2 activation, Cell Chemical Biology (2023), https://doi.org/10.1016/j.chembiol.2023.07.014

CellPress

STAR★METHODS

KEY RESOURCES TABLE

REAGENT or RESOURCE	SOURCE	IDENTIFIER
Antibodies		
TUBG1	Sigma	RRID: AB_477584
FLAG	Sigma	M2 RRID: AB_259529
NRF2	Proteintech	RRID: AB_2881867
Succinyl lysine	PTM Biolabs	RRID: AB_2937058
MYC	Bethyl laboratories	RRID: AB_2891453
KEAP1	Santa Cruz Biotech	RRID: AB_10844829
Mouse IgG2b control	CST	RRID: AB_2799435
Chemicals, peptides, and recombinant proteins		
Succinic anhydride	Sigma Aldrich	Cat#239690
Succinic anhydride alkyne	Enamine	EN200-172303
GSH	Sigma Aldrich	Cat#458139
Vitamin E	Sigma Aldrich	Cat#5.00878
DCFDA	Sigma Aldrich	Cat#21884
MitoTempo	Sigma Aldrich	Cat# EN200-172303
ET-29	MedChemExpress	Cat#HY-145651
Poly-d-lysine	Thermo Fisher	Cat#A3890401
Optimem	Gibco	Cat#31985062
Fugene	Promega	Cat#E2311
Polybrene	Sigma Aldrich	Cat#TR-1003-G
FLAG peptide	Sino biological	Cat#PP101274
Galactose	Sigma Aldrich	Cat#G5388
Protease inhibitor	Roche	Cat#11697498001
Puromycin	Thermo Fisher	Cat#A1113803
Coomassie	Biorad	Cat#161-0803
RIPA	Millipore	Cat#20188
Apo Horseradish Peroxidase	Calzyme	Cat# 239A0000
Hydrogen Peroxide	Sigma Aldrich	Cat#H1009
Amplex UltraRed	Invitrogen	Cat#A36006
CM-H2DCFDA	Invitrogen	Cat#C6827
Critical commercial assays		
Q5 Site Directed Mutagenesis Kit	NEB	Cat#E0554S
BrightGlo luciferase assay system	Promega	Cat# E2610
RNeasy kit	Qiagen	Cat#74004
SuperScript III First Strand Synthesis Kit	Invitrogen	Cat#18080051
TB Green Advantage qPCR premix	Takara Bio	Cat#639676
GTPase-Glo Assay	Promega	Cat#V7681
CellTiter-Glo Luminescent Cell Viability Assay	Promega	Cat#G75573
Anti FLAG magnetic beads	Thermo Fisher	Cat#M8823
Protein A/G magnetic beads	Pierce	Cat#88802
Experimental models: Cell lines		
K562	ATCC	Cat#CCL-234
HEK293T	ATCC	Ca#CRL-3216
IMR32	ATCC	Cat#CCL-127

(*Continued on next page*)

Please cite this article in press as: Ibrahim et al., Succinylation of a KEAP1 sensor lysine promotes NRF2 activation, Cell Chemical Biology (2023), https://doi.org/10.1016/j.chembiol.2023.07.014

Continued

REAGENT or RESOURCE	SOURCE	IDENTIFIER
Oligonucleotides		
Human NQO1 ARE for pGF1 cloning	IDT	CTCAGCCTTCCAAATCGCAGT CACAGTGACTCAGCAGAAT
Tubulin forward primer	IDT	ATCTGCCTCCCGGTCTATG
Tubulin reverse primer	IDT	TACCTGTCGGAACATGGAGG
SUCLG2 forward primer	IDT	GTGGTATCGTCAACTGTGCC
SUCLG2 reverse primer	IDT	TCTTGGACGTTGGTTCCTTCA
NQO1 forward primer	IDT	GCCTCCTTCATGGCATAGTT
NQO1 reverse primer	IDT	GGACTGCACCAGAGCCAT
Recombinant DNA		
pGreenFire	System Biosciences	Cat#TR0XX
KEAP1-FLAG	Addgene	Cat#28023
MYC-NRF2	Addgene	Cat#21555
psPAX2	Addgene	Cat#11260
pMD2.G	Addgene	Cat#12259
Non-targeting control vector	Sigma Aldrich	SHC002
KEAP1	Sigma Aldrich	TRCN0000154656
FH	Sigma Aldrich	TRCN0000052463
TALDO1	Sigma Aldrich	TRCN0000052519
TKT	Sigma Aldrich	TRCN0000054073
CS	Sigma Aldrich	TRCN0000045703
SUCLG2-1	Sigma Aldrich	TRCN0000048503
SUCLG2-2	Sigma Aldrich	TRCN0000048505
NRF2	Sigma Aldrich	TRCN0000007555
Software and algorithms		
GraphPad ver 9	Prism	RRID:SCR_002798
Flowjo v10.3	BD Biosciences	RRID:SCR_008520

RESOURCE AVAILABILITY

Lead contact

Further information and requests for resources and reagents used in this study should be directed to the lead contact, Michael Bollong (mbollong@scripps.edu).

Materials availability

All cell lines, plasmids, and other stable reagents generated in this study are available from the lead contact with a completed Materials Transfer Agreement.

Data and code availability

- Any data reported in this paper will be shared by the lead contact upon request.
- This paper does not report original code.
- Any additional information required to reanalyze the data reported in this paper is available from the lead contact upon request.

EXPERIMENTAL MODELS AND STUDY PARTICIPANT DETAILS

Cell lines

K562, HEK293T, and IMR32 cells were purchased from American Type Culture Collection (ATCC). K562 cells (human, female, chronic myelogenous leukemia) were maintained in RPMI (Corning) supplemented 10% with fetal bovine serum (FBS, Gibco) and 1% penicillin-Streptomycin (Pen Strep, Gibco). HEK293T (human, female, embryonic kidney) and IMR32 cells (human, male, neuroblastoma) were maintained in DMEM (Corning) supplemented 10% with fetal bovine serum (FBS, Gibco) and 1% penicillin-Streptomycin (Pen Strep, Gibco). For experiment with galactose media, cells were grown in DMEM (no glucose) supplemented

Please cite this article in press as: Ibrahim et al., Succinylation of a KEAP1 sensor lysine promotes NRF2 activation, Cell Chemical Biology (2023), https://doi.org/10.1016/j.chembiol.2023.07.014

with 10 mM galactose for 1 week. All cells were maintained at 37°C in 5% CO2 in a humidified incubator according to ATCC's recommendations.

METHOD DETAILS

Cloning

To generate the ARE-GFP-LUC vector, the ARE sequence from the human NQO1 promoter, synthesized as double stranded synthetic DNA oligo (IDT), was inserted between the EcoR1 and BglII sites in pGreenFire. To generate KEAP1-FLAG mutants, single- and double-point mutations (C151S/A, K131A) were introduced into FLAG-KEAP1 using primers synthesized by IDT and a Q5® Site-Directed Mutagenesis Kit.

Lentivirus production and transduction

Lentiviruses were generated in HEK293T cells by transient expression of the indicated shRNA vectors below with psPAX2 and pMD2.G packaging vectors. For lentiviral production in 96 well plates, $1.5*10^4$ HEK293T cells were plated in poly-d-lysine coated wells in 100 μL of growth medium. Transfection mixtures contained 30 μL of Optimem medium 100 ng of shRNA, psPAX2, and pMD2.G each, and 1μg total DNA:4μL of Fugene per well. Viral supernatants were collected after 48 h of expression and added to target cells with the addition of a final concentration of 5 μg/mL polybrene).

Stable cell line production

48 hrs after transduction of K562 cells with lentiviruses encoding the ARE-GFP-LUC construct, cultures were exposed to 5 μg/mL of puromycin for one week. Single cells were then plated in 96 well plates and allowed to expand for several weeks. The monoclonal line with the most dynamic and reproducible increase in FITC+ signal by flow cytometry after shKEAP1 transduction (tested at 48, 72, and 96 hrs post-transduction) was selected for use in the screen.

shRNA screen in ARE-GFP-LUC K562 reporter cells

ARE-GFP-LUC K562 reporter cells ($2*10^4$ in 50 μL) were dispensed into 96 well plates and transduced as described above with 100 μL of lentiviral shRNAs. After 72 hrs cells were analyzed for GFP positivity using a NovoCyte 3000 with NovoSampler Pro.

ARE-LUC reporter assays

IMR32 cells were plated in 40 μL of growth medium (5000 cells/well) in white 384-well plates (Greiner). The next day each well was transfected with 100 ng pTI-ARE-LUC using FuGENE HD (4 μL per ug DNA) in freshly filtered 10 μL OptiMEM medium, or 50 ng of the reporter and 50 ng of shRNA. For experiments with KEAP1-FLAG mutants, 20 ng of MYC-NRF2 was included in the transfection mix. 24 hrs later compounds (antioxidants or SA/SA-alkyne) were added in 10 μL of 6x solutions. After treatment (24 hrs for antioxidants, 4 hrs for SA/SA-alkyne), 30 μL BrightGlo (diluted 1:3 in water) were dispensed to each well, plates shaken for one minute, and the luminescence signal recorded using an Envision plate reader (PerkinElmer).

qRT-PCR

Treated HEK293T cells were collected from 6 well plates via trypsinization. RNA was isolated using RNeasy kits and concentrations quantified using a Nanodrop instrument. 2 μg of RNA was then subjected to oligo dT-primed reverse transcription reactions. Quantitative RT-PCR reactions were measured on a Viia7 Instrument (Thermo) using Clontech SYBR green-based master mix. Calculations were normalized using TUBG1 (Tubulin) as a reference. Ct values were determined using the Viia7 software and transcript abundance was calculated using the standard comparative Ct method.

Quantification of ROS by DCFDA fluorescence

K562 cells were plated in 96-well plates and treated/transduced as previously described. Cells were then washed and resuspended in DPBS. CM-H2DCFDA was freshly dissolved in DMSO. Cells were incubated in 5 μM CM-H2DCFDA for 30 min and analyzed on a NovoCyte 3000.

KEAP1-FLAG labeling experiments in HEK293T cells

6-well tissue culture plates were coated with poly-d-lysine, and $5*10^5$ HEK293T cells were plated per well. Wells were transfected with 1 μg of the indicated KEAP1 encoding vectors with 4 μL Fugene HD in 0.1 mL Opti-MEM (and additional 1 μg for shSUCLG2 experiments with 8 μL Fugene HD total). After a 48 hr incubation cells were treated with the indicated concentration of SA/SA-alkyne for 1 hr. For competition experiment, cells were exposed to SA for 1 hr after initial incubation with alkyne probe. For experiment with shSUCLG2, cells were treated with ET-29 24 hrs after transfection. Cells were washed with cold PBS twice, scraped in 0.25 mL RIPA buffer containing protease inhibitor, and lysed by sonication. Insoluble materials were removed by centrifugation (13,000 g for 5 minutes at room temperature). 1 mg of lysate was immunopurified with 20 μL of M2 Anti-FLAG magnetic beads and FLAG tagged material eluted using an excess of FLAG peptide in 50 μL. Similar procedure for co-immunoprecipitation of MYC-CUL3 with KEAP1-FLAG was followed, except without sonication. Samples were mixed with loading buffer and separated by SDS-PAGE followed by immunoblotting. For MS/MS-based proteomics, the gel was stained with Coomassie and the band containing

Please cite this article in press as: Ibrahim et al., Succinylation of a KEAP1 sensor lysine promotes NRF2 activation, Cell Chemical Biology (2023), https://doi.org/10.1016/j.chembiol.2023.07.014

KEAP1 was excised and submitted. For experiments with SA-alkyne, the FLAG elute from the steps above was incubated with click reagent mix (1 μL of 1.25 mM rhodamine azide in DMSO, 1 μL of 50 mM CuSO4 in H2O, 1 μL of 50 mM TCEP in water, 3 μL of 1.7 mM TBTA in tBuOH:DMSO 4:1) at room temperature for 1 hr in the dark. The reaction mixture was precipitated in cold methanol and the pellet was re-dissolved in PBS containing 0.1% SDS. The resulting sample was mixed with loading buffer and separated via SDS-PAGE. Gels were incubated in 10% EtOH for 1 hr before imaging fluorescence on a ChemiDoc instrument (Bio-Rad).

Recombinant KEAP1 labeling *in vitro*

KEAP1 was reconstituted in PBS containing 30% glycerol to a final concentration of 2 mg/mL. 1 μg KEAP1 in 50 μL PBS was incubated with the indicated concentrations of SA/succinyl coA at 37°C for 1 hr, and then samples resolved by SDS-PAGE followed by Coomassie staining. The band containing KEAP1 was excised and submitted for MS/MS-based proteomics.

Immunoblotting

Cells were collected by scraping in 250 μL ice cold 1x RIPA buffer with protease inhibitor. Lysates were sonicated using a tip sonicator (Branson) followed by clearing of insoluble material by centrifugation. The protein concentration of the supernatants was estimated by absorbance measurements on a Nanodrop instrument. 30 μg of lysate per lane was resolved using 4-12% Bis-Tris SDS PAGE gels (Invitrogen) and then transferred to PVDF membrane (Bio-Rad). Membranes were blocked in 5% non-fat dry milk (Biorad) in TBST (Tris-buffered saline with 0.1% Tween 20) for 1 hr at room temperature. Primary antibodies were incubated in milk in TBST overnight at 4°C. Primary antibodies used here were anti-TUBG1 (1:2000), FLAG (1:2000), anti-NRF2 (1:2000), anti-succinyllysine (1:1000), anti-MYC and anti-SUCLG2 (1:2000). After 5x TBST washes for 15-30 minutes, fluorophore-conjugated (1:2000, LI-COR) or HRP-conjugated (1:3000, ThermoFisher) secondary antibodies were incubated in milk for 1 hr and then washed again with TBST before visualizing on a LI-COR Odyssey fluorescent scanner or with film.

Endogenous KEAP1 immunoprecipitation

HEK293T cells were plated, treated, and collected as described above. Lysate (2 mg/mL in 200 μL) was precleared with 20 μL of protein Pierce protein A/G magnetic beads. 5 μg of anti-KEAP1 or anti-mouse IgG2b control was added to the lysate and incubated overnight at 4°C. The following day, 20 μL of protein A/G beads were added and incubated with shaking for 3 hrs at 4°C. After washing with lysis buffer, samples were boiled in 0.1% SDS and separated by SDS-PAGE.

Quantification of cellular ATP, GTP, and heme

HEK293T cells stably transduced with non-targeting vector or shRNAs targeting SUCLG2 were collected by scraping into PBS. Tip sonication, followed by centrifugation at 14,000 x g yielded lysates that were normalized using absorbance measurements at 280 nm. For GTP quantification, 1 mg of each lysate in 1 mL of PBS was incubated with 5U of apyrase (NEB) for 2 hours at room temperature before inactivating enzyme for 10 minutes at 95°C. 20 μL of each reaction was incubated with GTPase glo mix (Promega, V7681) for 5 minutes at room temperature before the addition of 40 μL of detection reagent (Promega, V7681) in white 384-well plates (Corning). Luminance values were recorded on an Envision microplate reader after a 10-minute incubation at room temperature with shaking. For ATP quantification, 10 μg of lysate in 20 μL of PBS was dispensed to each well of a white 384-well plate (Corning) before the addition of 20 μL of CellTiterGlo reagent (diluted 1:6 in water). For quantification of labile heme, 5 μL of apo-HRP (25 nM solution; Calzyme) was incubated in black 384-well plates (Corning) with 5 μL of lysate (10 μg total, prepared as above) for five minutes at room temperature. 40 μL of 0.1 M phosphate buffer containing 50 μM Amplex UtraRed (Invitrogen), 0.02% hydrogen peroxide (Sigma) was then added to each well. Fluorescence (excitation at 490 nm; emission at 585 nm) was then recorded on a Spectramax iD3 instrument (Molecular Devices).

QUANTIFICATION AND STATISTICAL ANALYSIS

Statistics were calculated in PRISM 9 (GraphPad, San Diego, CA). Data are presented as mean +/− SD and were analyzed by the student t-test or one- or two-way ANOVA, as indicated in the accompanying figure legends.

Cell Chemical Biology, Volume *30*

Supplemental information

Succinylation of a KEAP1 sensor lysine promotes NRF2 activation

Lara Ibrahim, Caroline Stanton, Kayla Nutsch, Thu Nguyen, Chloris Li-Ma, Yeonjin Ko, Gabriel C. Lander, R. Luke Wiseman, and Michael J. Bollong

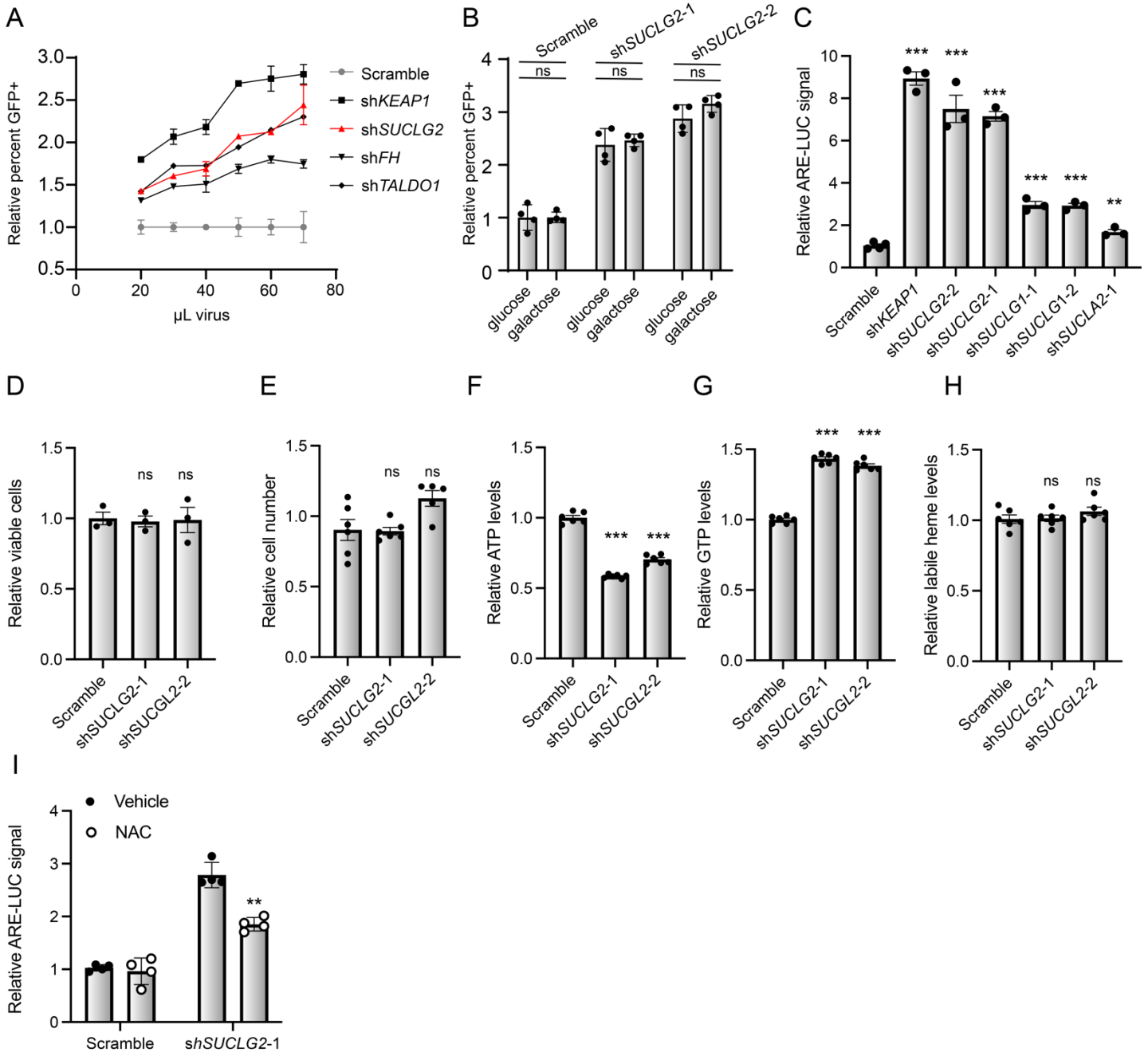

Supplementary Figure 1. Knockdown of *SUCLG2* activates ARE-GFP-LUC, related to Figure 1. A) Relative ARE activation from ARE-GFP-LUC K562 cells in response to the indicated volumes of lentiviruses encoding the indicated shRNAs. B) Relative ARE activation from ARE-GFP-LUC K562 cells in response to treatment with lentiviruses encoding the indicated shRNAs to *SUCLG2* grown in either glucose or galactose (*n*=4). C) Relative ARE activation from HEK293T cells transfected with shRNAs targeting KEAP1 or or the indicated SCS components SUCLG2, SUCLG1, or SUCLA2 (*n*=3; mean and s.d.). Relative viable ARE-GFP-LUC K562 cells in response to treatment with lentiviruses encoding shRNAs to *SUCLG2* as determined by flow cytometry (*n*=3; mean and s.d.). Relative cell number (E), ATP levels (F), GTP levels (G), and labile heme levels (H) from HEK293T cells transduced with shRNAs targeting SUCLG2 (*n*=6; mean and s.d.). (I) Relative ARE activation from HEK293T cells transduced with shRNAs targeting SUCLG2 and treated with N-acetyl cysteine (NAC, 10 mM; *n*=4; mean and s.d.; ns = not significant $P>0.05$, $^{**}P<0.005$, $^{***}P<0.005$, two-way ANOVA).

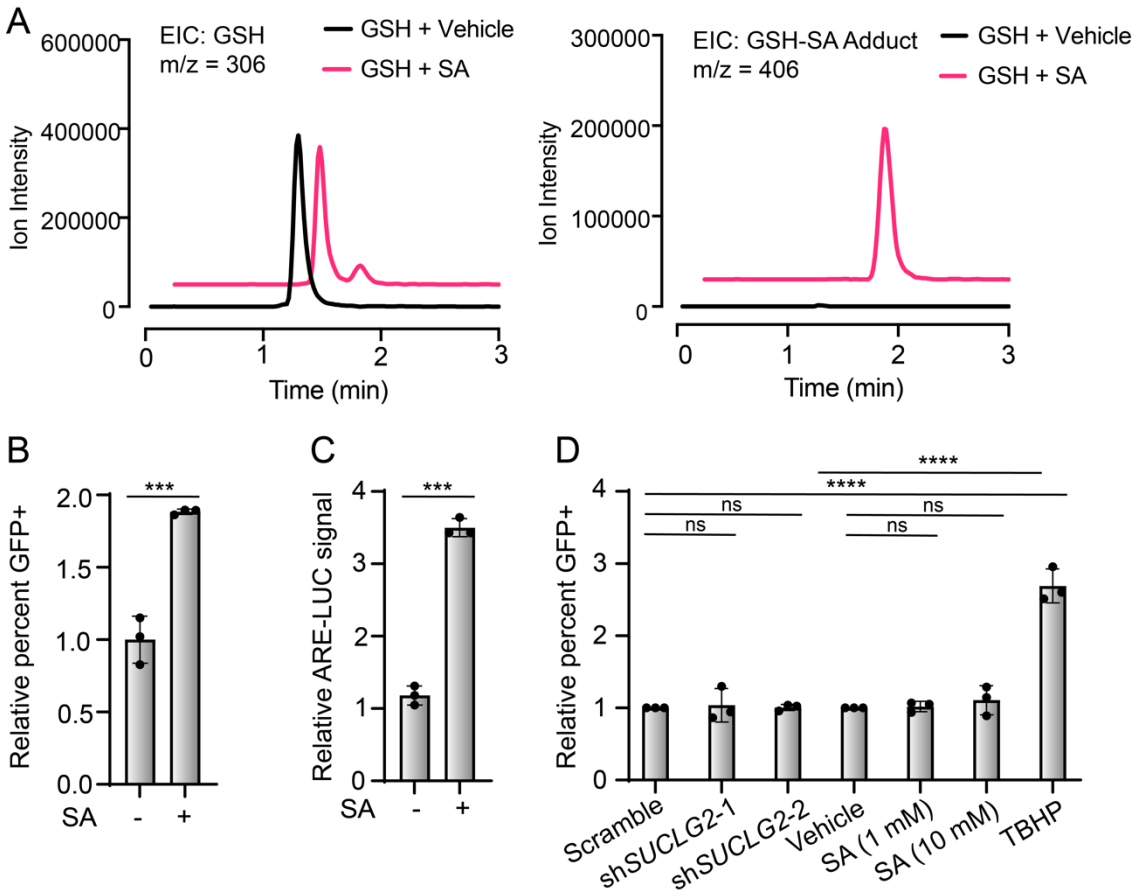

Supplementary Figure 2. SA activates ARE-GFP-LUC in K562 cells, related to Figure 2. A) Extracted ion chromatograms corresponding to GSH (left) and the GSH-SA adduct (right) from in vitro reactions containing GSH with or without (SA). B) Relative percent GFP positive K562 ARE-GFP-LUC cells after treatment with 50 mM SA for 4 hrs (*n*=3; mean and s.d.; ***P<0.001, t-test). C) Relative luminescence signal of reporter activity from K562 ARE-GFP-LUC cells after treatment with 50 mM SA for 4 hrs (*n*=3; mean and s.d.; ***P<0.001, t-test). D) Relative percent GFP positive measurements indicating the presence of reactive species from K562 cells treated with virus expressing shRNAs targeting *SUCLG2* or treatment with the indicated compounds (TBHP = tert-butyl hydro peroxide; *n*=3, mean and s.d.; ns = not significant P>0.05, ****P<0.0001, one-way ANOVA).

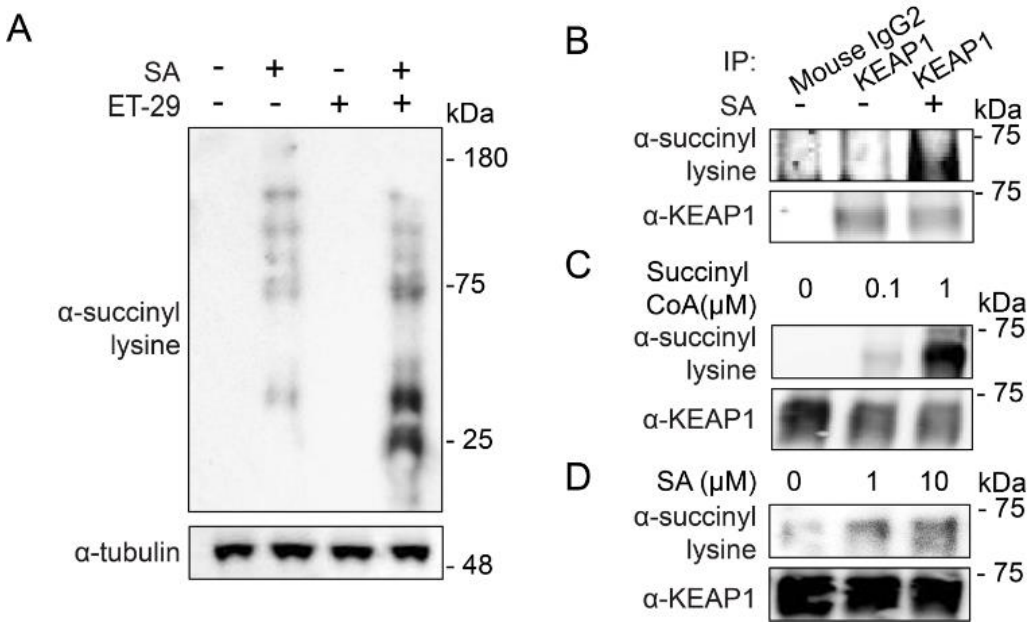

Supplementary Figure 3. Covalent modification of KEAP1 lysines in response to SA, related to Figure 3. A) Western blotting analysis for anti-succinyl lysine positivity after treatment of HEK293T cells with ET-29 (10 μM) and SA (5 mM, 1 hr). B) Western blotting anti-succinyl lysine positivity from pulldowns of endogenous KEAP1 from HEK293T cells treated with SA (5 mM, 1 hr). Western blotting anti-succinyl lysine positivity of recombinant KEAP1 after a 1 hr in vitro treatment with the indicated concentrations of succinyl-CoA (C) or SA (D).

A

#	b	b^{++}	b*	b*$^{++}$	b^{0}	b^{0++}	Seq.	y	y^{++}	y*	y*$^{++}$	y^{0}	y^{0++}	#
1	130.0499	65.5286			112.0393	56.5233	E							19
2	258.1084	129.5579	241.0819	121.0446	240.0979	120.5526	Q	2139.0573	1070.0323	2122.0307	1061.519	2121.0467	1061.027	18
3	315.1299	158.0686	298.1034	149.5553	297.1193	149.0633	G	2010.9987	*1006.003*	1993.9722	997.4897	1992.9881	996.9977	17
4	446.1704	223.5888	429.1438	215.0756	428.1598	214.5836	M	1953.9772	977.4923	1936.9507	968.979	1935.9667	968.487	16
5	575.213	288.1101	558.1864	279.5969	557.2024	279.1049	E	1822.9368	*911.972*	1805.9102	903.4587	1804.9262	902.9667	15
6	674.2814	337.6443	657.2549	329.1311	656.2708	328.6391	V	1693.8942	*847.4507*	1676.8676	838.9374	1675.8836	838.4454	14
7	773.3498	387.1785	756.3233	378.6653	755.3393	378.1733	V	*1594.8258*	*797.9165*	1577.7992	789.4032	1576.8152	788.9112	13
8	860.3818	430.6946	843.3553	422.1813	842.3713	421.6893	S	*1495.7573*	*748.3823*	1478.7308	739.869	1477.7468	739.377	12
9	973.4659	487.2366	956.4394	478.7233	955.4553	478.2313	I	*1408.7253*	704.8663	1391.6988	696.353	1390.7147	695.861	11
10	1102.5085	551.7579	1085.482	543.2446	1084.4979	542.7526	E	*1295.6412*	*648.3243*	1278.6147	639.811	1277.6307	639.319	10
11	1159.53	580.2686	1142.5034	571.7553	1141.5194	571.2633	G	*1166.5987*	*583.803*	1149.5721	575.2897	1148.5881	574.7977	9
12	1272.614	636.8107	1255.5875	628.2974	1254.6035	627.8054	I	*1109.5772*	555.2922	1092.5506	546.779	1091.5666	546.287	8
13	1409.6729	705.3401	1392.6464	696.8268	1391.6624	696.3348	H	*996.4931*	*498.7502*	979.4666	490.2369	978.4826	489.7449	7
14	1506.7257	753.8665	1489.6992	745.3532	1488.7151	744.8612	P	*859.4342*	430.2207	842.4077	421.7075	841.4237	421.2155	6
15	1734.8367	867.922	1717.8102	859.4087	1716.8261	858.9167	K	762.3815	381.6944	745.3549	373.1811	744.3709	372.6891	5
16	1833.9051	917.4562	1816.8786	908.9429	1815.8946	908.4509	V	*534.2704*	267.6389	517.2439	259.1256	516.2599	258.6336	4
17	1964.9456	982.9764	1947.9191	974.4632	1946.935	973.9712	M	*435.202*	218.1047	418.1755	209.5914	*417.1915*	209.0994	3
18	2093.9882	1047.4977	2076.9617	1038.9845	2075.9776	1038.4925	E	304.1615	152.5844	287.135	144.0711	286.151	143.5791	2
19							R	*175.119*	88.0631	158.0924	79.5498			1

B

#	b	b^{++}	b*	b*$^{++}$	b^{0}	b^{0++}	Seq.	y	y^{++}	y*	y*$^{++}$	y^{0}	y^{0++}	#
1	130.0499	65.5286			112.0393	56.5233	E							19
2	258.1084	129.5579	241.0819	121.0446	240.0979	120.5526	Q	2155.0522	1078.0297	2138.0257	1069.5165	2137.0416	1069.0245	18
3	315.1299	158.0686	298.1034	149.5553	297.1193	149.0633	G	2026.9936	*1014.0005*	2009.9671	1005.4872	2008.9831	1004.9952	17
4	462.1653	231.5863	445.1388	223.073	444.1547	222.581	M	1969.9722	985.4897	1952.9456	976.9764	1951.9616	976.4844	16
5	591.2079	296.1076	574.1814	287.5943	573.1973	287.1023	E	1822.9368	*911.972*	1805.9102	903.4587	1804.9262	902.9667	15
6	690.2763	345.6418	673.2498	337.1285	672.2658	336.6365	V	1693.8942	*847.4507*	1676.8676	838.9374	1675.8836	838.4454	14
7	789.3447	395.176	772.3182	386.6627	771.3342	386.1707	V	*1594.8258*	*797.9165*	1577.7992	789.4032	1576.8152	788.9112	13
8	876.3768	438.692	859.3502	430.1787	858.3662	429.6867	S	*1495.7573*	*748.3823*	1478.7308	739.869	1477.7468	739.377	12
9	989.4608	495.2341	972.4343	486.7208	971.4503	486.2288	I	*1408.7253*	704.8663	1391.6988	696.353	1390.7147	695.861	11
10	1118.5034	559.7553	1101.4769	551.2421	1100.4929	550.7501	E	1295.6412	*648.3243*	*1278.6147*	639.811	1277.6307	639.319	10
11	1175.5249	588.2661	1158.4983	579.7528	1157.5143	579.2608	G	*1166.5987*	*583.803*	1149.5721	575.2897	1148.5881	574.7977	9
12	1288.6089	644.8081	1271.5824	636.2948	1270.5984	635.8028	I	*1109.5772*	555.2922	1092.5506	546.779	1091.5666	546.287	8
13	1425.6679	713.3376	1408.6413	704.8243	1407.6573	704.3323	H	*996.4931*	*498.7502*	979.4666	490.2369	978.4826	489.7449	7
14	1522.7206	761.8639	1505.6941	753.3507	1504.7101	752.8587	P	*859.4342*	*430.2207*	842.4077	421.7075	841.4237	421.2155	6
15	1750.8316	875.9195	1733.8051	867.4062	1732.8211	866.9142	K	762.3815	381.6944	745.3549	373.1811	744.3709	372.6891	5
16	1849.9	925.4537	1832.8735	916.9404	1831.8895	916.4484	V	*534.2704*	267.6389	517.2439	259.1256	516.2599	258.6336	4
17	1980.9405	990.9739	1963.914	982.4606	1962.93	981.9686	M	*435.202*	218.1047	418.1755	209.5914	417.1915	209.0994	3
18	2109.9831	1055.4952	2092.9566	1046.9819	2091.9726	1046.4899	E	304.1615	152.5844	287.135	144.0711	286.151	143.5791	2
19							R	*175.119*	88.0631	158.0924	79.5498			1

C

#	b	b^{++}	b*	b*$^{++}$	b^{0}	b^{0++}	Seq.	y	y^{++}	y*	y*$^{++}$	y^{0}	y^{0++}	#
1	130.0499	65.5286			112.0393	56.5233	E							19
2	258.1084	129.5579	241.0819	121.0446	240.0979	120.5526	Q	2155.0522	1078.0297	2138.0257	1069.5165	2137.0416	1069.0245	18
3	315.1299	158.0686	298.1034	149.5553	297.1193	149.0633	G	2026.9936	*1014.0005*	2009.9671	1005.4872	2008.9831	1004.9952	17
4	462.1653	231.5863	445.1388	223.073	444.1547	222.581	M	1969.9722	985.4897	1952.9456	976.9764	1951.9616	976.4844	16
5	591.2079	296.1076	574.1814	287.5943	573.1973	287.1023	E	1822.9368	*911.972*	1805.9102	903.4587	1804.9262	902.9667	15
6	690.2763	345.6418	673.2498	337.1285	672.2658	336.6365	V	1693.8942	*847.4507*	1676.8676	838.9374	1675.8836	838.4454	14
7	789.3447	395.176	772.3182	386.6627	771.3342	386.1707	V	*1594.8258*	*797.9165*	*1577.7992*	789.4032	1576.8152	788.9112	13
8	876.3768	438.692	859.3502	430.1787	858.3662	429.6867	S	*1495.7573*	*748.3823*	1478.7308	739.869	1477.7468	739.377	12
9	989.4608	495.2341	972.4343	486.7208	971.4503	486.2288	I	*1408.7253*	704.8663	1391.6988	696.353	1390.7147	695.861	11
10	1118.5034	559.7553	1101.4769	551.2421	1100.4929	550.7501	E	1295.6412	*648.3243*	*1278.6147*	639.811	1277.6307	639.319	10
11	1175.5249	588.2661	1158.4983	579.7528	1157.5143	579.2608	G	*1166.5987*	*583.803*	1149.5721	575.2897	1148.5881	574.7977	9
12	1288.6089	644.8081	1271.5824	636.2948	1270.5984	635.8028	I	*1109.5772*	555.2922	1092.5506	546.779	1091.5666	546.287	8
13	1425.6679	713.3376	1408.6413	704.8243	1407.6573	704.3323	H	*996.4931*	*498.7502*	979.4666	490.2369	978.4826	489.7449	7
14	1522.7206	761.8639	1505.6941	753.3507	1504.7101	752.8587	P	*859.4342*	*430.2207*	842.4077	421.7075	841.4237	421.2155	6
15	1750.8316	875.9195	1733.8051	867.4062	1732.8211	866.9142	K	762.3815	381.6944	745.3549	373.1811	744.3709	372.6891	5
16	1849.9	925.4537	1832.8735	916.9404	1831.8895	916.4484	V	534.2704	267.6389	517.2439	259.1256	516.2599	258.6336	4
17	1980.9405	990.9739	1963.914	982.4606	1962.93	981.9686	M	435.202	218.1047	418.1755	209.5914	417.1915	209.0994	3
18	2109.9831	1055.4952	2092.9566	1046.9819	2091.9726	1046.4899	E	304.1615	152.5844	287.135	144.0711	286.151	143.5791	2
19							R	*175.119*	88.0631	158.0924	79.5498			1

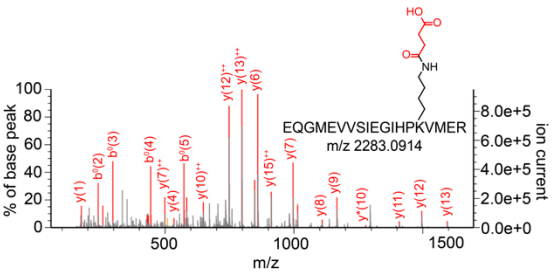

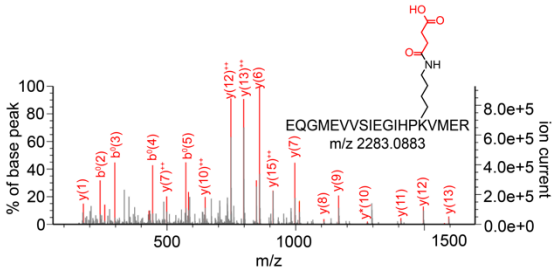

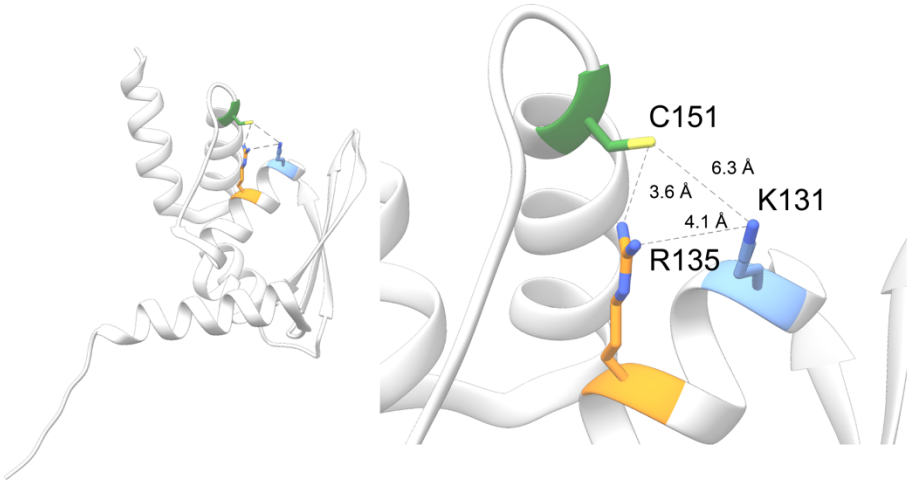

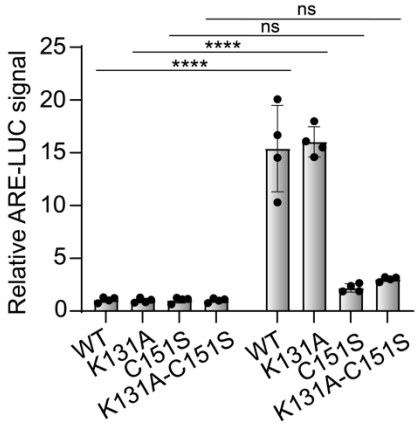

Supplementary Figure 4: Lysine 131 of KEAP1 is covalently modified by SA, related to Figure 4. A) *b* and *y* ion designations corresponding to MS/MS spectra in Figure 4A. B,C) *b* and *y* ion designations (left) and MS/MS spectra (right) corresponding to +101 Da modified tryptic KEAP1 peptides K131 from 1 hr *in vitro* reactions of SA (10 mM (A) and 1 mM (B)) with recombinant KEAP1. C) Representation of the BTB domain of KEAP1 (left; PDB: 4CXI) with inset denoting orientations of key residues K131, R135, and C151 (right). D) ARE-luciferase reporter activity of IMR32 cells expressing the indicated KEAP1 transgene mutants after treatment with 500 nM bardoxolone methyl for 24 hrs (*n*=4; mean and s.d.; ns = not significant P>0.05, ****P<0.0001, two-way ANOVA).